Electronic processes in double-barrier resonant-tunneling structures studied by photoluminescence spectroscopy in zero and finite magnetic fields

M. S. Skolnick, D. G. Hayes,* P. E. Simmonds,*,† A. W. Higgs, G. W. Smith, H. J. Hutchinson, and C. R. Whitehouse
Royal Signals and Radar Establishment, Saint Andrews Road, Great Malvern, Worcestershire WR14 3PS, United Kingdom

L. Eaves, M. Henini, O. H. Hughes, M. L. Leadbeater, and D. P. Halliday
Department of Physics, University of Nottingham, Nottingham NG7 2RD, United Kingdom
(Received 2 October 1989; revised manuscript received 29 January 1990)

Clear evidence for space-charge buildup and the occurrence of sequential tunneling processes, in GaAs-$Ga_{1-x}Al_xAs$ double-barrier resonant-tunneling structures, is obtained from photoluminescence investigations in zero and finite magnetic fields. The charge densities in the quantum-well regions are determined from zero-field line-shape fits and the study of Landau-level intensities as a function of magnetic field. The occurrence of sequential tunneling in structures with two quasiconfined electron subbands is demonstrated from the spectroscopic observation of large charge densities in the lower subband, when the structures are biased for tunneling into the upper electronic level. The temperature of the electronic charge which builds up in the quantum wells at the two resonances is determined from the line-shape-fitting procedures.

I. INTRODUCTION

Double-barrier resonant-tunneling structures (DBRTS's) were first discussed and demonstrated in 1973–1974.[1] However, it is only in the last few years that a significant amount of study has been directed towards a proper understanding of the fundamental physical processes which take place in DBRTS's. These include the question of whether tunneling is predominently coherent or sequential,[2] and the magnitudes and consequences of space-charge buildup in the quantum-well (QW) part of the structure on resonance.[3,4] Such an understanding is particularly important given the large number of potential applications for such structures, for example in the fields of high-speed electronics[5] and multivalued logic devices.[6]

In two recent publications, Young and co-workers[7,8] have employed low-temperature photoluminescence (PL) to investigate characteristics of the resonant-tunneling process. They deduced, from these results, values for the charge buildup, which occurs on resonance, and for the variation of tunneling rates with applied bias. However, the validity of the charge-density determination in the quantum well in Ref. 7, obtained from the variation of PL intensity with applied bias suitably scaled to the charge density expected at zero bias, has been questioned and further discussed in a recent Comment and Reply.[9,10]

In the present paper, a detailed photoluminescence study of the electronic transport processes in two DBRTS's, containing two quasibound electronic subbands, is reported. The observation of band-filling effects on the PL linewidth, as a function of applied bias, is shown to provide direct evidence for charge buildup in the quantum-well parts of the structures at the two resonances. The occurrence of charge buildup is additionally demonstrated by the observation of Landau-level splittings of the PL lines as a function of applied magnetic field. A direct measure of the charge density in the well is obtained from the field at which the quantum limit is reached in the PL spectra. The relative degrees of electron energy relaxation, before tunneling out of the well occurs, at the resonances, is analyzed from a study of the Landau-level populations as a function of magnetic field. Very clear evidence for the importance of sequential tunneling processes is obtained from the observation of PL from electrons in the lower subband when the devices are biased at the second electron resonance. Evidence that the tunneling at the first resonance is also sequential in the present structures is obtained from the study of Landau-level populations as a function of applied bias. Preliminary accounts of some of the results discussed here have been presented in Refs. 11 and 12.

The paper is organized in the following way. In the next section details of the structures and of the experimental photoluminescence setup are described. Then in Sec. III the variation of the PL spectra with applied bias is discussed, with particular emphasis being paid to deduction of the charge densities in the wells on resonance from line-shape fitting of the PL spectra. In Sec. IV, spectroscopic evidence for the occurrence of sequential tunneling in the structures under investigation is presented, followed in Sec. V by studies of the PL spectra in magnetic field, and finally in Sec. VI the main conclusions of the paper are summarized.

II. EXPERIMENTAL DETAILS

The experiments were carried out on two GaAs-$Ga_{1-x}Al_xAs$ DBRTS's grown by molecular-beam epitaxy (MBE), the details of which are given in Table I. Structure 1 contains a GaAs QW of 58-Å width and asymmetric $Ga_{0.6}Al_{0.4}As$ barriers with 83- and 111-Å widths, in addition to the usual n^+ GaAs contact layers

 ©1990 The American Physical Society

TABLE I. Sample characteristics.

Composition	Structure 1	Structure 2
n-type GaAs contact	0.5 μm, 2×10^{18} cm^{-3} 500 Å, 1×10^{17} cm^{-3} 500, Å, 1×10^{16} cm^{-3}	0.25 μm, 1×10^{18} cm^{-3} 0.75 μm, 2×10^{17} cm^{-3}
GaAs	33 Å	102 Å
$Ga_{1-x}Al_xAs$	$x=0.4$, 111 Å	$x=0.33$, 85 Å
GaAs	58 Å	79 Å
$Ga_{1-x}Al_xAs$	$x=0.4$, 83 Å	$x=0.33$, 85 Å
GaAs	33 Å	102 Å
n^+ GaAs contact	500 Å, 1×10^{16} cm^{-3} 500 Å, 1×10^{17} cm^{-3} 2.0 μm, 2×10^{18} cm^{-3}	0.5 μm, 2×10^{17}, cm^{-3} 0.5 μm, 1×10^{18} cm^{-3}
n^+ GaAs substrate	2×10^{18} cm^{-3}	4×10^{17} cm^{-3}

and spacer layers.[13] The incorporation of a thicker "collector" barrier, for electron transport in the direction from the substrate to the top contact (defined as reverse bias, top contact positive), leads to strong charge buildup in the well on resonance and to the occurrence of intrinsic bistability due to the resulting large electrostatic feedback.[14–20] A PL investigation of the intrinsic bistability phenomena is presented elsewhere.[11] The electrical characteristics of structure 1 were first described in Refs. 17, 18, and 19 where the evidence that the bistability is intrinsic in nature was discussed in full. However, the principal arguments that support this interpretation are that the bistability is only observed for the bias direction in which strong charge buildup occurs, and that the current-voltage characteristics are independent of external circuit parameters, in contrast to the behavior expected in the case of extrinsic, load-line-controlled bistability. For further discussion, see Refs. 17, 18, and 19. Structure 2 is a symmetric DBRTS with a GaAs QW width of 79 Å and equal $Ga_{0.67}Al_{0.33}As$ barrier widths of 85 Å. Both structures contain two quasibound electron states and exhibit two negative-differential-resistance features for both bias directions. 200-μm mesas were employed for the PL experiments, with either annular contacts, or circular contacts smaller than the mesa size, being employed for the optical measurements. PL was excited in the low intensity limit to minimize perturbation to the I-V characteristics, with ~0.2 W/cm^2 of the 632.8-nm line of a He-Ne laser, dispersed with a 0.75-m spectrometer, and detected with a cooled GaAs photomultiplier. Magnetic field experiments were performed in the Faraday configuration, in a 10-T superconducting magnet. All the work reported here was carried out with the samples directly immersed in liquid helium at 2 K.

III. RESULTS AND DISCUSSION OF ZERO-MAGNETIC-FIELD EXPERIMENTS

A. Structure 1

The current-voltage (I-V) characteristics of structure 1, taken under the weak illumination conditions employed for the PL measurements, are shown in Fig. 1(a) for reverse applied bias (V) (top contact positive). Two negative-differential-resistance (NDR) features and bistable regions, at -0.68 to -0.7 V and -2.4 to -2.44 V (discussed in Refs. 17–19), are visible. The variation of PL peak position, linewidth (full width at half maximum) at zero magnetic field and 9.6 T, and integrated PL intensity with bias, are presented in Figs. 1(a)–1(d), respectively. An important result for the present paper is the strong correlation between the variation of tunnel current [Fig. 1(a)] and PL linewidth at $B=0$ T [Fig. 1(b)] with reverse bias. This result will be discussed in detail later, where it will be shown to arise from the effect on the PL linewidth of charge buildup in the well during resonant tunneling. The PL intensity (Fig. 1) on the other hand does not show any clear correlation with the I-V characteristics, except at the onset of tunneling at ~0.2 V, in contrast to the results presented by Young *et al.*[7] PL studies under forward bias where very little charge buildup occurs, and a reasonable correlation between the PL intensity and current variations with bias is found, will be discussed briefly at the end of Sec. III A. Actual PL spectra, from which the results of Fig. 1 are obtained, are shown in Fig. 2 at particularly significant bias values.

A schematic diagram of the conduction- and valence-band profiles, when biased at the first resonance, is shown in Fig. 3. At this resonance, electrons tunnel from the two-dimensional electron-gas (2D EG) accumulation layer in the emitter contact into the lower subband in the QW, where charge buildup occurs, before they tunnel out through the thicker second barrier into the collector.

The PL spectra in Fig. 2 arise from recombination between carriers in the lowest electron and heavy-hole states in the GaAs QW part of the structure. There is a strong shift of the PL peak positions to lower energy with applied bias, as plotted in Fig. 1(a) of 20 meV at -3.3 V. This shift arises from the quantum confined Stark effect[21] and is close to the value expected for a 60-Å QW in an electric field of 2.3×10^5 V/cm. At $V=0$, the PL arises predominantly from direct electron-hole creation in the QW and subsequent recombination. A weak PL band, with a tail to the low-energy side, is observed at $V=0$

[Fig. 2(a)]. As soon as the tunnel current starts to flow [at $V=-0.23$ V, Fig. 1(a)], the PL line becomes symmetric, narrower, probably due to the saturation of defect- or impurity-related PL processes [Figs. 1(b) and 2(b)], and the peak shifts to lower energy by ~ 2.5 meV [Fig. 1(a)]. A similar shift of the PL spectrum to lower energy, and narrowing of the PL line, near the onset of current flow is reported later for structure 2 and has also been observed earlier by Young *et al.*[8] It should be noted that in addition to the PL signals from the GaAs QW part of the structure, which form the main subject of the present paper, strong PL from the n^+ GaAs contact regions, ~ 500 times stronger than that from the QW is also observed.

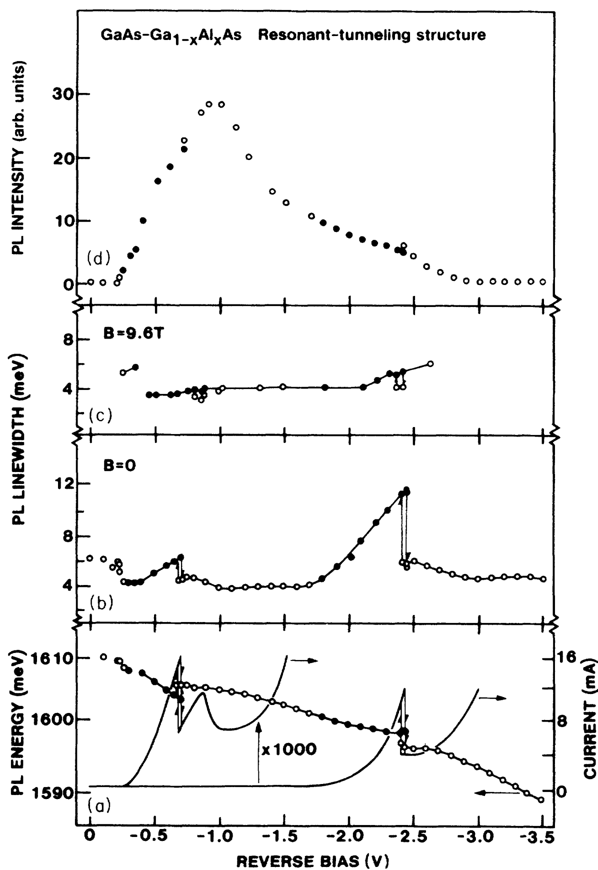

FIG. 1. Current [solid line, panel (a)], PL peak position [circles, panel (a)], PL linewidth (full width at half maximum) at $B=0$ and 9.6 T [(b) and (c), respectively], and integrated PL intensity [panel (d)] as a function of applied reverse bias for structure 1. The solid and open circles in (a)–(d) represent on and off resonance states, respectively. Two resonances and associated negative-differential-resistance regions are observed in the I-V characteristics. At both resonances the structure is bistable with associated hysteresis loops being observed in current, PL peak position, and linewidth. The variation of PL linewidth with bias in (b) shows a strong correlation with that of the I-V characteristics and arises from the variation of charge stored in the well with bias. In magnetic field, (c), the free-carrier broadening effects on the PL linewidth are removed.

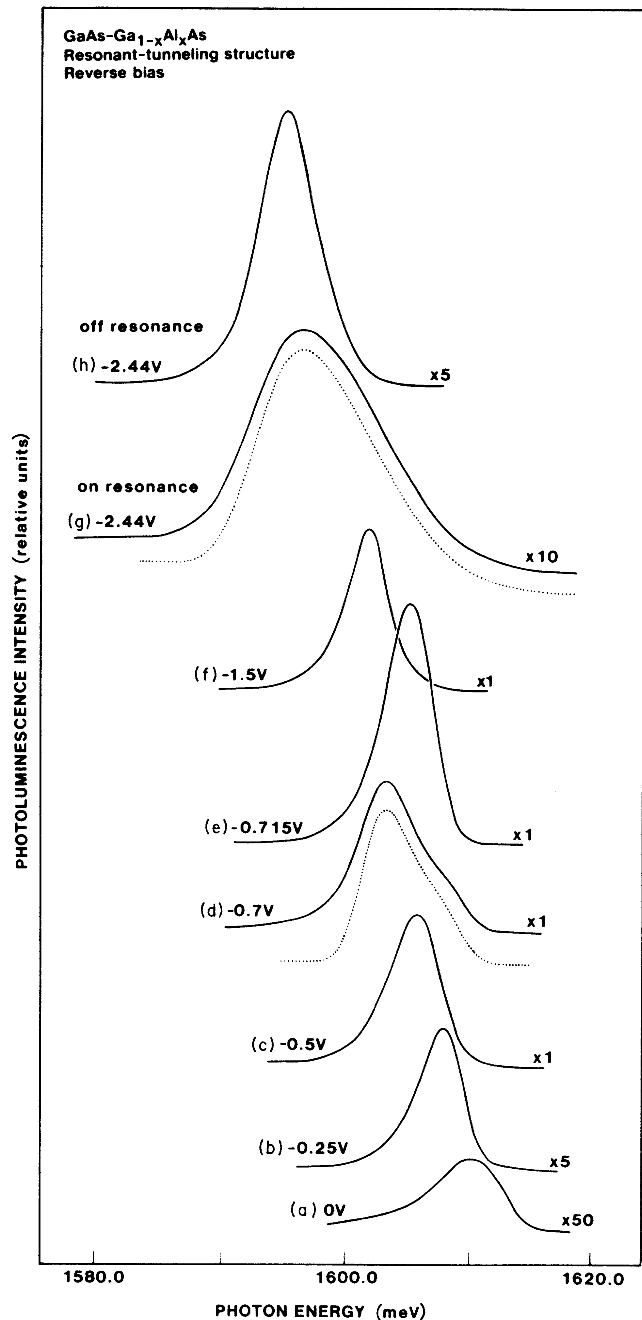

FIG. 2. PL spectra as a function of reverse bias for structure 1. The asymmetric line observed at $V=0$ [(a)] is replaced by a sharper, symmetric peak as soon as tunnel current flows [(b), $V=-0.25$ V]. With increasing bias at the first resonance charge builds up in the well, and the PL line broadens with increasing bias [(c) and (d)] until the structure switches to the low-current state at -0.715 V [(e)]. The onset of the second resonance at occurs at ~ -1.7 V, and charge buildup increases up to the peak of the resonance at -2.44 V [(g)]. The bistable behavior of the structure is seen by comparison of the spectra of (g) and (h) both taken at -2.44 V, but in low- and high-current states, respectively. The Fermi cutoff is marked on (d). The dotted curves below (d) and (g) are line-shape fits to the spectra on resonance.

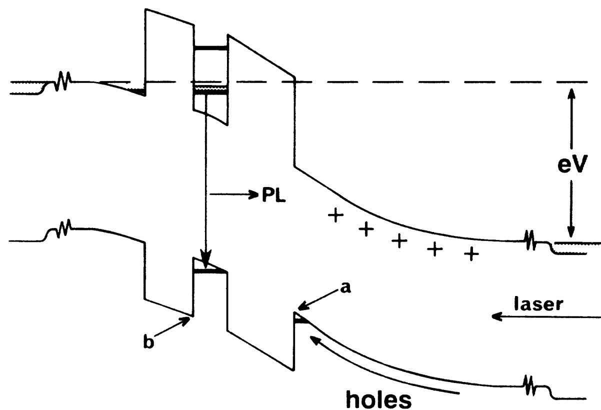

FIG. 3. Schematic diagram of conduction- and valence-band profiles for structure 1, biased at the first resonance at ~ -0.65 V. Electrons tunnel from the accumulation layer in the emitter contact into the quantum well, where charge buildup occurs. The holes are generated predominantly in the "collector" (for electrons) region, and form an accumulation layer at the collector barrier, before tunneling into the well and recombining with the much higher density of electrons. At $V \approx -0.9$ V, $V_a \approx V_b$, and the onset of the decrease of the hole collection rate in the QW occurs.

With increasing applied bias, within the first resonance, the tunnel current increases strongly [Fig. 1(a)], the PL linewidth increases nearly linearly [Figs. 1(b) and 2(a)–2(c)] and there is a very strong increase in PL intensity [Fig. 1(c)]. Under applied bias, and on a tunneling resonance the PL arises from recombination of the tunneling electrons, whose density in the well builds up with increasing tunnel current, (density $n_s^e \sim 2.2 \times 10^{11}$ cm^{-2} at -0.7 V, large compared to the photocreated electron density of $\leq 10^9$ cm^{-2}) and holes which are photocreated principally in the GaAs contact region.[22] Under the influence of the applied bias, these holes accumulate at the thick $Al_xGa_{1-x}As$ "collector" barrier, where they form a 2D hole gas, and subsequently tunnel into the well.[23] The density of the holes, (n_s^h) at the collector barrier under the illumination conditions employed is estimated to be $\sim 10^{10}$ cm^{-2} from the small perturbation of the *I-V* characteristics of 20 mV to lower bias observed under illumination. This value of n_s^h is obtained from a calculation of the extra electric field required across the barrier-well-barrier region of the structure to give rise to the observed 20-mV shift of the *I-V* characteristics. The hole density in the well must be less than this, possibly in the range 10^8 to 10^9 cm^{-2} given likely hole tunneling rates into the well, but the actual value will be dependent on the applied bias. An upper limit for the hole density in the well of 10^9 cm^{-2} is also obtained from the electron-hole pair generation rate in the structure, estimated from an incident laser power of 0.2 W/cm^2 and a minority carrier lifetime of 1 nsec.

We have demonstrated the dominance of hole creation in the GaAs in giving rise to the observed PL *under applied bias,* from PL excitation (PLE) spectra of the QW PL.[22] These PLE spectra show only very weak excitation features due to transitions between the confined hole and electron levels in the QW. The dominance of hole creation processes in the GaAs contact regions is also demonstrated by the fact that the QW PL can be excited at photon energies below the QW band gap.[22,23] Such photons can only excite electron-hole pairs in the GaAs. The holes then tunnel into the QW and recombine with the electrons which have built up in the well because of the tunneling process.

The marked increase in linewidth from 4.2 to 6.2 meV between -0.4 and -0.7 V on the first resonance [Figs. 1(b) and 2(b)–2(d)] arises from build up of space charge in the well with increasing tunnel current. PL spectra arising from the recombination between a high density of electrons in a QW and photocreated thermalized holes have been recently investigated in some detail.[24–28] The electrons populate states from the bottom of the conduction band (wave vector $k=0$) up to the electron Fermi energy E_F ($=h^2 n_s^e/4\pi m^*$). In high-quality QW's the oscillator strength for recombination is expected to fall off towards E_F due to wave-vector restrictions, at a rate which is determined by the degree of disorder (or degree of hole localization) in the system. This general description accounts well for the behavior observed in Fig. 2(d). The spectrum peaks on the low-energy side, decreases towards higher energies, and shows a cutoff at the Fermi energy, as indicated on Fig. 2(d). When the bias voltage is increased slightly beyond -0.7 V, the structure goes off resonance [Fig. 1(a)], charge buildup in the well is strongly reduced, and a much narrower, nearly symmetric PL line is observed [Fig. 2(e)].

The change in line shape between the on and off resonance states can be used to deduce the magnitude of the space-charge buildup in the well. Such a determination is complicated by the contribution of both free-carrier and inhomogeneous effects to the observed, asymmetric PL line shape on resonance. Nevertheless, by convolving the line shape observed at the onset of the first resonance (at -0.3 V, where $n_s^e \approx 0$) with a Fermi function, together with a decreasing oscillator strength towards E_F, a good fit, shown by the dotted curve below the spectrum of Fig. 2(d), can be obtained. A value for E_F at the peak of the first resonance of 7.5 ± 1.0 meV is obtained from this fit, and hence an n_s^e value of $(2.2 \pm 0.3) \times 10^{11}$ cm^{-2}, for $m^* = 0.07 m_0$, is deduced. The reliability of this determination is strongly aided by the observation of a clear feature in Fig. 2(d) at the electron Fermi energy. This value for n_s^e agrees with that determined from magneto-PL measurements at -0.7 V, from the magnetic field at which the quantum limit is attained (as discussed in detail later), and with the value $n_s^e = 2 \times 10^{11}$ cm^{-2} obtained from oscillatory magneto capacitance studies on the same structure by Leadbeater *et al.*[18-19]

The electron Fermi energy as a function of bias cannot be deduced directly from the PL linewidth versus V results of Fig. 1(b) due to the strongly asymmetrical line shapes observed, without the carrying out of a fitting procedure of the type discussed above. Nevertheless, the strong increase of linewidth with tunnel current is a clear

signature of charge buildup in the well at both resonances. Further confirmatory evidence of the contribution of band-filling effects to the increase of PL linewidth on resonance is provided by the magneto-PL measurements.

Beyond the cutoff of the first resonance, a peak in the I-V characteristics at -0.87 V arising from LO-phonon-assisted resonant tunneling[29,30] is observed [Fig. 1(a)]. Such inelastic processes also lead to charge buildup in the well as seen in Fig. 1(b), by the small increase of the PL linewidth from -0.7 to -0.75 V and subsequent decrease up to -1.0 V, to a value of 3.8 meV. The onset of the second resonance occurs at -1.7 V, and is accompanied once again by a strong increase in PL linewidth up to the large value of 11.8 meV at -2.44 V [Figs. 1(b) and 2(g)].

A line-shape fitting to the spectrum at the second resonance and deduction of E_F are less reliable than that carried out for the first resonance due to the absence of a feature at the Fermi energy in the spectrum. The broad high-energy tail to the spectrum can only be explained if the temperature of the electrons is in the range 25 to 40 K. The elevated electron temperature is the reason for the absence of a Fermi-energy feature in the spectrum. The deduction of a high carrier temperature is further substantiated by the magnetic field experiments presented in Sec. V B. An n_s^e value of 3.2×10^{11} cm^{-2} ($E_F=11$ meV) at -2.4 V is deduced from the magnetic field studies. A good fit to the spectrum of Fig. 2(g) is obtained for this value of E_F, involving a convolution of the off resonance line shape at -2.44 V [Fig. 2(h)] with a Fermi function at $T=25$ K and once again a decreasing oscillator strength towards E_F, and is shown by the dotted curve in Fig. 2(g).

For the second resonance, the magnetic field experiments are very important in the determination of a reliable value for n_s^e. However, it should be noted that the strong increase of linewidth between -1.8 and -2.4 V and the "convex" shape of the spectrum in Fig. 2(g) to higher energy beyond the PL peak at 1597 meV provide clear evidence for the presence of a high-density electron gas in the QW, whose density increases with applied bias. If instead n_s^e were close to zero, it would not be possible to explain the shape of the spectrum in Fig. 2(g) between 1597 and 1607 meV from a fitting to a nondegenerate Boltzmann distribution for $T\approx25$ to 40 K, since in this case the shape of the curve in this region would always be concave, in disagreement with experiment.

As discussed earlier, the structure exhibits intrinsic bistability,[14–20] and accompanying hysteresis loops at the two NDR features in its I-V characteristics [Fig. 1(a)]. Similar phenomena are observed in the PL results, with both the PL linewidth [Fig. 1(b)] and peak position [Fig. 1(a)] exhibiting bistable behavior and hysteresis. These results are presented in more detail in Ref. 10. The bistability is clearly demonstrated from a comparison of Figs. 2(g) and 2(h) where two spectra taken at -2.44 V are shown. For Fig. 2(g), the biasing condition is approached from low reverse bias; the structure is in its high-current state, with the result that the large PL linewidth of 11.8 meV is observed. In Fig. 2(h), the -2.44-V condition is approached from the direction of high bias. The structure is then in its low-current state, little charge is stored in the well, and a relatively narrow PL linewidth of 6 meV is observed.

Young and co-workers[7] deduced values for the charge density in the well at resonance from the variation of PL intensity with applied bias. In their structure there was a reasonably good correlation between the variations of integrated PL intensity and tunnel current with bias. In the present work on structure 1 in reverse bias, such a correlation is found only at the onset of current flow of the first resonance at ~-0.2 V [compare Figs. 1(a) and 1(d)]. The PL intensity in Fig. 1(d) increases rapidly at the onset of the first resonance, but then peaks at -0.95 V, within the phonon-assisted sideband of the first resonance,[29,30] and subsequently shows a smooth decrease down to -3.0 V to a value similar to that found at $0<|V|<0.2$ V. Only a very small change in PL intensity is observed at the switching point of the second resonance.

The factors which control the PL intensity (I_{PL}) will be discussed in more detail elsewhere,[22] but for the present publication the main point is that I_{PL} can depend on both the electron and hole densities (n_s^e,n_s^h) in the well.[7] For a fixed hole collection rate in the QW, I_{PL} is proportional to n_s^e if the hole decay rate is dominated by nonradiative processes,[7] which include hole tunneling out of the well. Thus, the strong increase of I_{PL} at -0.2 V can be accounted for by the increase of n_s^e in the well as tunnel current starts to flow. However, as n_s^e increases beyond $\sim2\times10^{10}$ cm^{-2}, radiative recombination of holes quickly becomes dominant, and the PL intensity will be independent of n_s^e, since any competing nonradiative decay channel now makes a negligible contribution to the total hole recombination rate. This condition is expected to hold from about -0.4 V to the cutoff of the second resonance at -2.44 V. It should be noted that even between the resonances in reverse bias, electron charge builds up in the well due to elastic, and to LO-phonon-assisted inelastic tunneling, at a density $\sim5\times10^{10}$ cm^{-2}, which is enhanced by the presence of the thick collector barrier.[18] Under the above conditions of high radiative efficiency, the PL intensity will instead be controlled by the variation of n_s^h with bias.

At finite bias, most of the holes which participate in the PL are created in the GaAs contact region, as discussed above. They drift and diffuse to the thicker collector (for electrons) barrier, and with increasing bias up to ~-0.9 V they can tunnel with increasing probability into confined hole states in the well. However, when the potential drop across the collector barrier and QW becomes greater than the valence-band offset of ~160 mV (this corresponds to the potential of point b marked on Fig. 3 becoming higher than that of point a), an increasing fraction of the holes accumulated at the collector barrier will have sufficient potential energy to pass directly over the top of the second emitter barrier. This will lead to a strong reduction of the hole population in the well, and hence PL intensity, with further increase of bias. From a solution of Poisson's equation for the structure this condition is calculated to occur at V_{applied} of -0.9 V,

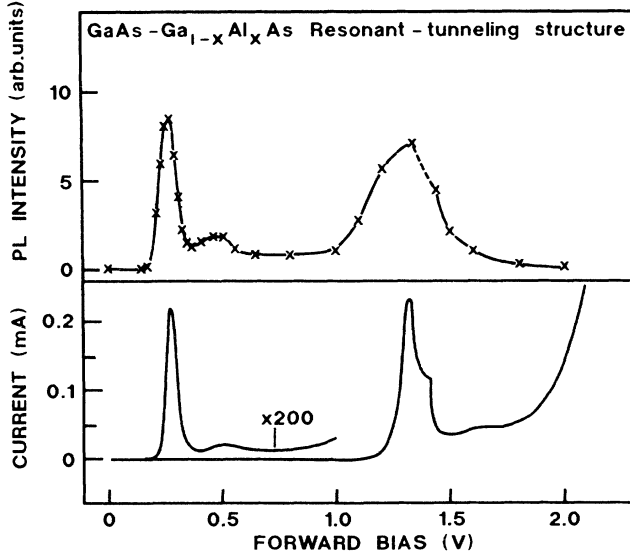

FIG. 4. Current (I) and integrated PL intensity (I_{PL}) variations as functions of applied forward bias for structure 1. In the upper part of the figure, the crosses are the experimentally observed PL intensities; the line drawn through them is a guide for the eye. Very little charge buildup occurs in the QW for this bias direction, since the electrons tunnel out of the QW through the thin AlGaAs barrier. A reasonably good correlation between I_{PL}, I vs V is observed. The structure is unstable at biases of 1.32 to 1.42 V beyond the second resonance. As a result the PL intensities in this region, drawn dashed, are not characteristic of a unique state of the device.

thus accounting well for the observed decrease in PL intensity beyond -0.95 V. This estimate neglects small errors which arise due to the confinement energy of ~ 30 meV of holes in the electrostatic potential at the collector barrier.

The conclusion to be drawn from these remarks is that care must be exercised in interpreting changes in PL intensity solely in terms of changes of n_s^e in the well. The variation of PL linewidth and line shape on resonance (and the magneto-PL analysis described in Sec. V) provide more clear-cut signatures of charge buildup in the well at resonance. In forward bias, on the other hand, where very little electron charge buildup in the well occurs since the electrons now tunnel out through the thin 83-Å barrier, the PL intensity versus bias shows a much closer correlation with the variation of current with voltage at the two resonances, as shown in Fig. 4. This is expected from the above considerations, since except within the second resonance, n_s^e is $\ll 2\times 10^{10}$ cm^{-2}, the hole recombination is dominated by nonradiative processes, and I_{PL} is controlled primarily by the variation of n_s^e with bias, as observed.

B. Structure 2

Structure 2 contains two quasibound electron subbands in its 79-Å QW and exhibits two resonances in its I-V

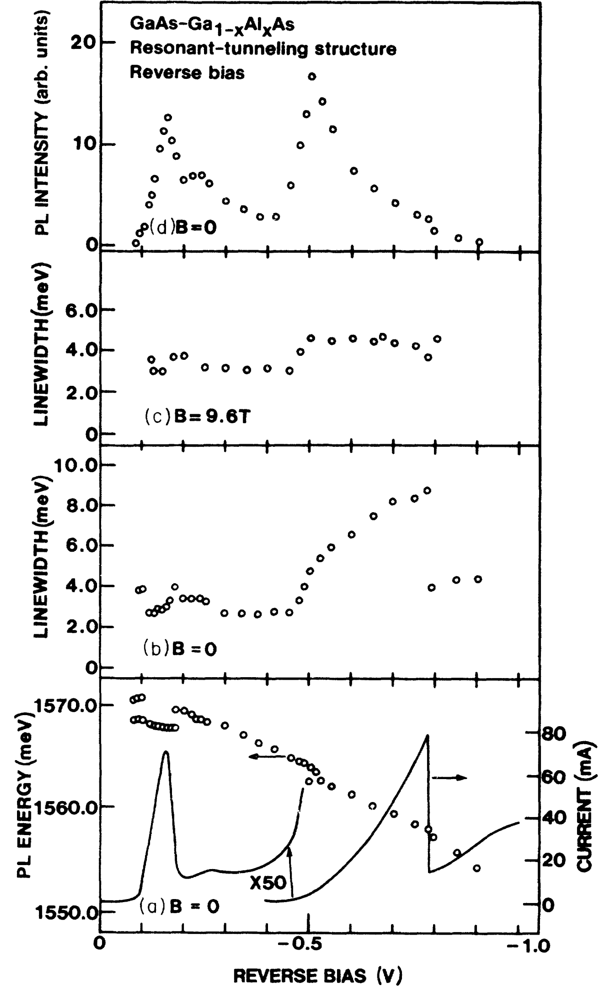

FIG. 5. As in Fig. 1, but for structure 2. Two tunneling resonances are again observed in the I-V characteristics. The increase of PL linewidth in panel (b) between -0.5 and -0.78 V indicates charge buildup in the well. The free-carrier contribution to the linewidth is removed by a quantizing magnetic field [panel (c)].

characteristics, as shown in Fig. 5(a) for reverse bias. The I-V characteristics are nearly symmetric between forward and reverse biases since the two $Al_xGa_{1-x}As$ barriers ($x = 0.33$) are of equal width in this case. The I-V measurements for the first resonance are taken with a 30-Ω resistor ($r \sim |dV/dI|$ in the NDR region) in parallel with the sample to suppress circuit oscillations which otherwise occur at this NDR feature. At the second resonance, the structure is stable without such external stabilization. Structure 1 does not exhibit such oscillations in reverse bias, but in forward bias at the second NDR features the structure is unstable[17,18] under normal circuit conditions (see Fig. 4).

The PL results for structure 2 are taken under stable conditions, in the manner described above, in all cases. The variations of PL peak position, linewidth at $B = 0$ and 9.6 T, and integrated PL intensity with applied reverse bias are presented in Figs. 5(a)–5(d), respectively,

and representative PL spectra are shown in Fig. 5. Qualitatively, the results contained in Figs. 5 and 6 are very similar to those described earlier for structure 1. A large Stark shift of the PL peak to lower energy of 16 meV at -0.9 V (at an electric field of 1.4×10^5 V/cm) is observed. The Stark shift is greater in the present case than for sample 1 because of the wider well width here (79 Å compared to 58 Å for structure 1). Once again at low bias before significant tunnel current flows an asymmetric PL line with a tail to lower energy is observed [Fig. 6(a) at -0.09 V]. When the voltage is increased to -0.15 V, the current increases strongly, and the PL line becomes symmetrical. There is only very little increase of the PL linewidth up to the peak of the first resonance, since the charge buildup in this structure, with symmetrical 85-Å barriers, is considerably less than in structure 1 with its 111-Å collector barrier. An upper limit for n_s^e at the peak of the first resonance of 5×10^{10} cm^{-2} can be obtained from the PL linewidth of 4 meV observed at -0.17 V. However, it should be noted that a complication arises in the analysis of the PL spectra at the first resonance due to the presence of two partially resolved peaks for $|V|<0.1$ V and $V=-0.18$ V [Figs. 5(a) and 6(b)]. The reason for the occurrence of two peaks at *low* n_s^e is not properly understood, but at least one of them probably arises from defect-related PL processes.

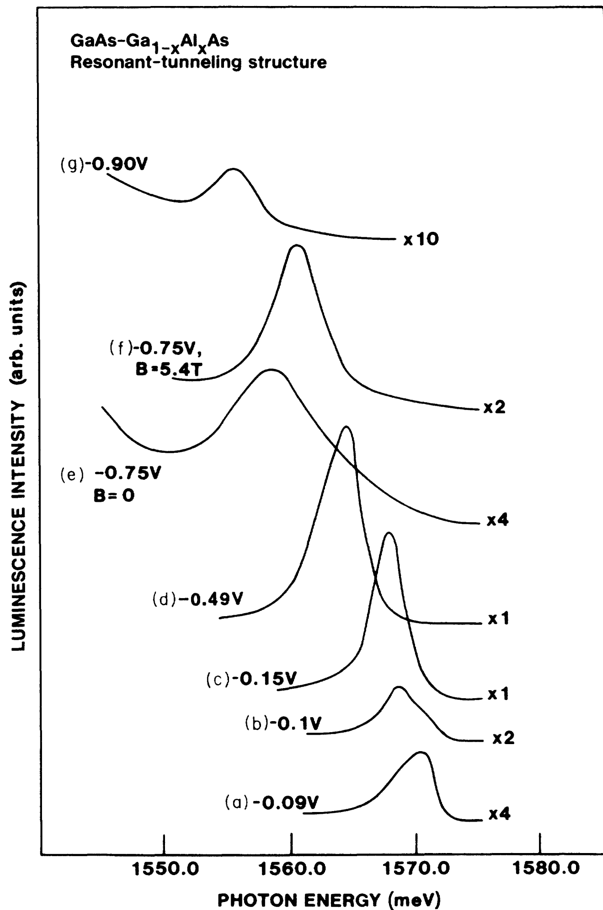

FIG. 6. PL spectra as a function of bias for structure 2. As for structure 1, the PL line shape at low bias is asymmetrical to the low-energy side [(a)]. This is replaced by a symmetrical sharper line as soon as significant tunnel current flows [(c), -0.15 V]. A strong increase in linewidth is observed within the second resonance from -0.5 to -0.78 V due to charge buildup in the well. Strong narrowing is observed at higher bias as charge is ejected from the well when the structure is again off resonance [(g), -0.9 V]. Figure (f) shows a spectrum at 5.4 T and -0.75 V near to the peak of the second resonance. The clear narrowing between (e) and (f) ($B=0$, and 5.4 T, respectively) shows that the $B=0$ spectrum is broadened by free-carrier effects. The sloping background at photon energies less than 1550 meV is due to PL from the doped GaAs contact layers.

At the onset of the second resonance at -0.45 V a marked increase in PL linewidth is observed. This increase continues to a value of 8.7 meV at the peak of the resonance at -0.78 V [see Figs. 5(a) and 6(e)], where the switch-down to the low-current state occurs. This increase in linewidth up to the peak of the second resonance is consistent with band filling by electrons whose density builds up in the well with increasing tunnel current. When the device switches to the low-current state beyond -0.78 V, a strong decrease in PL linewidth to ~4 meV occurs as the electronic charge is ejected from the well, in a very similar manner to that discussed for structure 1.

The determination of n_s^e at the second resonance from line-shape fitting is again complicated by the absence of a Fermi cutoff in the observed spectrum. However, a reasonable fit to the spectrum at -0.78 V, using the convolution procedure described earlier, can be obtained for $n_s^e=2\times10^{11}$ cm^{-2} and $T=30$ K. Further evidence for band filling, and a value for n_s^e are obtained from the magnetic field analysis in Sec. V B.

The variation of PL intensity with reverse bias in Fig. 5(d) is markedly different from that discussed earlier for structure 1 [Fig. 1(d)]. A reasonable correlation between I_{PL} versus V and the variation of tunnel current with bias is obtained at the first resonance in Fig. 5(d). As mentioned above for structure 1 and observed in forward bias for that structure in Fig. 4, such a correlation is expected in the low n_s^e regime, when the hole recombination is dominated by nonradiative processes. An approximate *upper* limit for n_s^e at the *peak* of the resonance at -0.17 V of 5×10^{10} cm^{-2} was obtained from the PL linewidth at this bias, qualitatively consistent with the conditions necessary to explain the correlation between I_{PL} and tunnel current. The distinction between the behavior of I_{PL} versus V for structures 1 and 2 in reverse bias arises because of the much higher n_s^e values for structure 1 due to the presence of the thick collector barrier which enhances charge buildup in the well.

For structure 2, I_{PL} increases again strongly at the onset of the second resonance at -0.45 V. However, it reaches its maximum value at -0.5 V, and then decreases at higher biases. This decrease arises due to a decrease of the hole collection in the QW with increasing bias above -0.4 V to -0.5 V, as shown in Fig. 7 where the conduction- and valence-band profiles obtained from

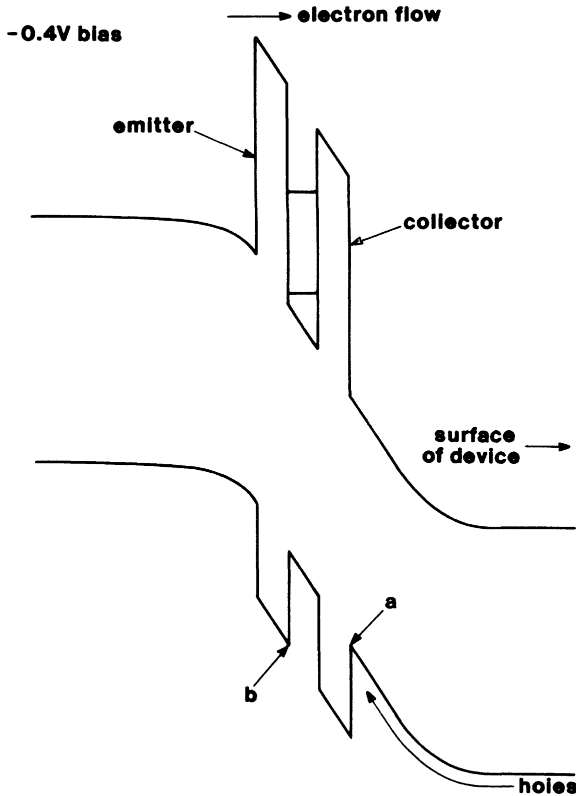

FIG. 7. Conduction- and valence-band diagram at -0.4 V for structure 2.

a solution of Poisson's equation at -0.4 V, are shown. This is the same phenomenon as that discussed for structure 1 at -0.9 V, when the potential drop across the "collector" barrier (for electrons) and the QW is equal to the valence-band offset, with the result that n_s^h and $I_{\rm PL}$ decrease with bias beyond -0.5 V. The peak at -0.25 V beyond the first resonance in Figs. 5(a) and 5(d) arises from LO-phonon-assisted inelastic tunneling.[29,30] It is not clear why it is more prominent in the $I_{\rm PL}$ versus V variation in Fig. 5(d) than in the I versus V curve of Fig. 5(a).

We have carried out tunneling resonance solutions of Schrödinger's equation for potential profiles of the type shown in Fig. 7, as a function of bias. These calculations predict Stark shifts of the electron 1 to heavy-hole 1 transition in good agreement (within 2 meV at -0.9 V) with the observed shift of the PL peak to lower energy in Fig. 5(a). They also show that $\sim 75\%$ of the observed shift occurs for the valence-band holes.

IV. EVIDENCE FOR SEQUENTIAL-TUNNELING PROCESSES

For both structures 1 and 2, the PL spectra presented in Figs. 2(g) and 2(h) and 6(e) and 6(f), at the second resonance, arise at the PL energy corresponding to recombination of electrons in the *lower* subband with holes in the first heavy-hole confined level in the valence-band well. We have been unable to detect any PL signal from electrons in the higher subband into which tunneling occurs from the emitter contact. These observations provide unambiguous *spectroscopic* evidence for the occurrence of sequential-tunneling processes[2] in these structures. Calculations of the tunneling rate (τ_t^{-1}) from the widths of the tunneling resonances for the *lower* subband, at -0.75 V for structure 2, give a value of $(\tau_t^{-1})_1 = 4.4\times 10^9$ sec^{-1}. In equilibrium the current density for transport out of the lower subband is given by $J = n_s^e e(\tau_t^{-1})_1 = 140$ A/cm^2 for $n_s^e = 2.0\times 10^{11}$ cm^{-2} estimated above. The value for J is close to that of 255 A/cm^2 observed at -0.75 V, consistent with the deduction that a substantial fraction ($\sim 50\%$ from the above comparison of J values) of the electrons undergo intersubband scattering, before tunneling out of the well. This implies that the intersubband scattering rate by LO-phonon emission [$\tau_i^{-1} \sim 10^{12}$ sec^{-1} (Refs. 31 and 32)] is of the order of the tunneling rate $(\tau_t^{-1})_2$ for electrons out of the upper subband. Calculations of $(\tau_t^{-1})_2$ are extremely sensitive to the conduction-band offset (280 meV) employed in the calculations since the second subband is close to the top of the collector barrier, so that the value we obtain of 10^{12} sec^{-1} may be in error by up to 1 order of magnitude. However, within these error limits, $(\tau_t^{-1})_2 \approx \tau_i^{-1}$ as required to be consistent with the importance of intersubband scattering in these structures. Similar results and conclusions regarding the importance of sequential tunneling at the second resonance apply also to structure 1.

V. MEASUREMENTS IN MAGNETIC FIELD RESULTS AND DISCUSSION

Strong evidence for space charge buildup in the wells at resonance, in addition to that presented from the linewidth results in Sec. III, is obtained from PL measurements in magnetic field. Such magneto-PL studies also permit more accurate values for n_s^e to be deduced than those obtained from the line-shape fitting, particularly for the second resonance (structure 1).

PL spectra for the first and second resonances at -0.68 and -2.40 V, respectively (high-current states for structure 1), as a function of magnetic field, are presented in Figs. 8 and 9. In both cases a splitting of the PL line into Landau levels (LL's) is observed. This is a clear signature of the contribution of free-carrier broadening[33] to the PL spectra on resonance at $B=0$. The degeneracy of an electron Landau level is given by $2eB/h$ including spin (spin splittings are not resolved experimentally), and thus increases linearly with magnetic field. So long as the LL splitting is greater than the inhomogeneous linewidth, LL structure should be observable in the PL spectra up to the field at which $n_s^e = 2eB/h$.[33] Above this field, the quantum limit is attained, the LL filling factor $\nu=2$, and all electrons can reside in the lowest LL. Thus, the determination of the field at which $\nu=2$ is reached permits a value for the charge density in the well, at resonance, to be obtained. Furthermore, in the quantum limit, with all electrons in the lowest LL, any free-carrier broadening of the PL spectrum is removed, thus enabling a separation to be made between the free-carrier and inhomogeneous

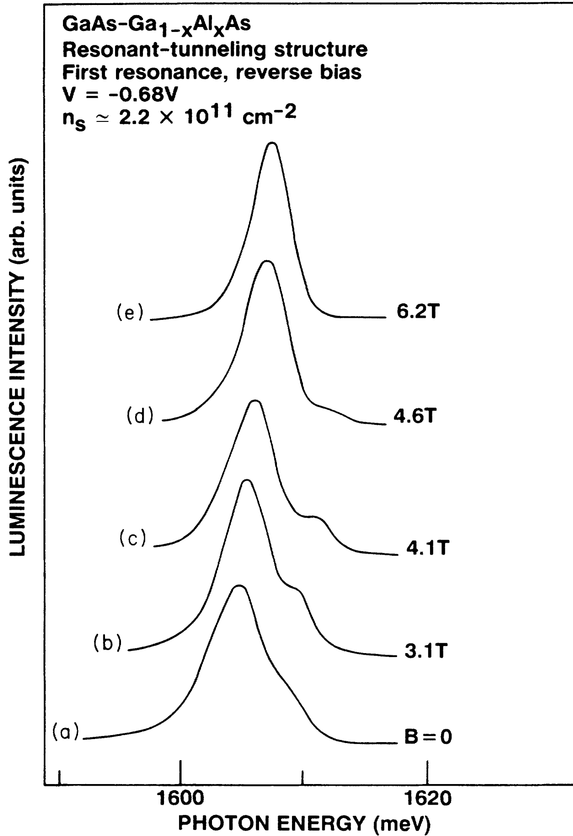

FIG. 8. PL spectra at first resonance at -0.68 V for structure 1, as a function of magnetic field. Splitting of the $B=0$ spectrum (a) into Landau levels (LL's) is observed. The $n=1$ LL depopulates at 4.65 T, at a filling factor of 2, from which a carrier density in the well of 2.2×10^{11} cm^{-2} is deduced.

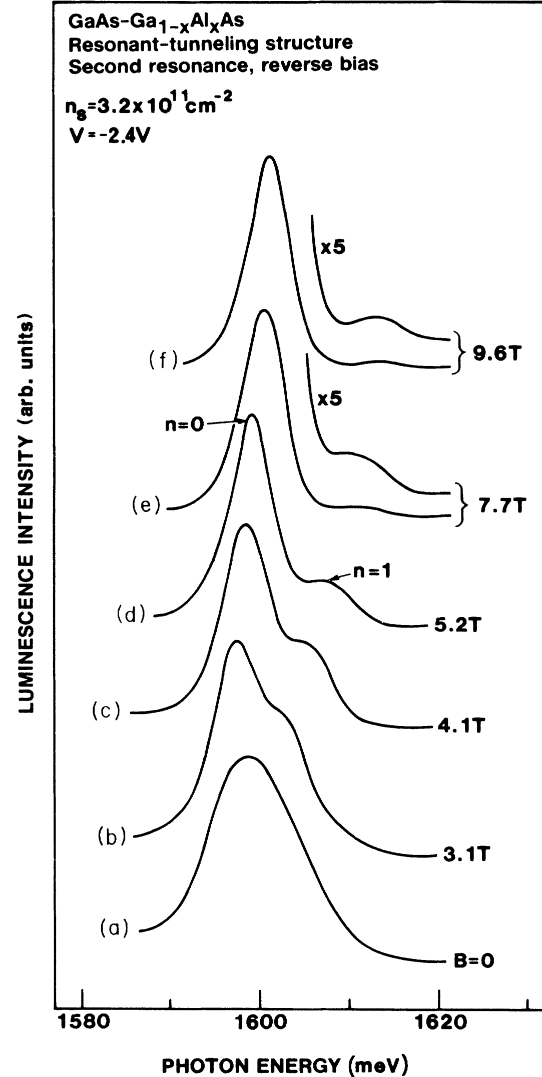

FIG. 9. PL spectra as a function of magnetic field at second resonance at -2.40 V for structure 1. As in Fig. 8 splitting into $n=0$ and 1 Landau levels is observed. A significant PL signal from the $n=1$ LL beyond $\nu=2$ at 6.7 T is observed ($I_1/I_0 \sim 0.022$ at 8.3 T), consistent with an electron temperature of $\sim$40 K in the lower subband.

broadening contributions to the $B=0$ spectra.

In the simplest case, the LL splitting should be given by the electron-cyclotron energy $\hbar\omega_c=\hbar eB/m_e^*$, where m_e^* is the electron effective mass. This is exactly as observed at the second resonance, where the observed splitting corresponds to $m_e^*=0.07m_0$, the low-energy electron effective mass in GaAs. This indicates that the same hole LL participates in the observed interband transitions. For the first resonance, on the other hand, a "reduced" effective mass of $0.1m_0$ is obtained from the observed LL splittings, probably because holes in higher LL's contribute to the observed transitions in this case.[34] We will now present a detailed analysis of the magnetic field results for the two resonances.

A. First resonance

To return to the spectra of Fig. 8 for the first resonance, splitting of the $B=0$ spectrum into $n=0$ and 1 LL's is observed. The $n=1$ LL is depopulated at a field of 4.65 T. By the methods discussed above ($n_s^e=2eB/h$ at $\nu=2$), a value for n_s of 2.2×10^{11} cm^{-2} is deduced, in agreement with the value obtained from the line-shape fitting. However, the value from the magnetic field studies is obtained in a more straightforward manner and does not involve any fitting procedure. The fact that a reduced mass of $0.1m_0$ is obtained from the splitting pattern, larger than the electron effective mass, does not detract from the reliability of the value of n_s^e obtained. The intensity of the $n=1$ LL peak as a function of field is controlled only by the population of electrons in this level. For example, if the bias voltage is decreased to reduce the charge in the well at fixed magnetic field (4.3 T) then the $n=1$ LL is observed to depopulate at a bias of -0.62 V, as shown in Fig. 10, demonstrating that its intensity is controlled by the electron population in the well.

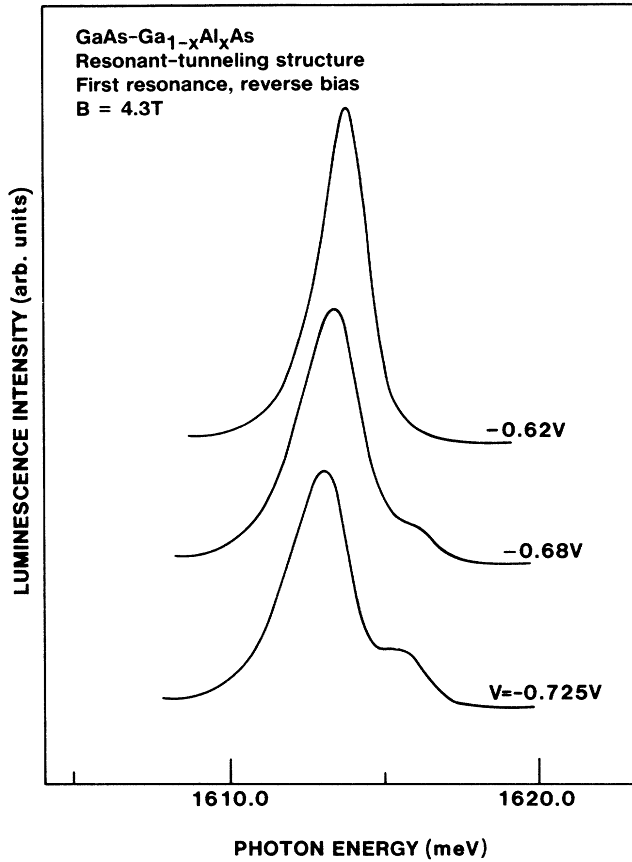

FIG. 10. PL spectra at 4.3 T for the first resonance of structure 1, as a function of bias. For a quantizing magnetic field, the bias at which the cutoff of the resonance occurs, increases, in this case to -0.725 V. As the reverse bias is reduced a decrease of population of the $n=1$ LL is observed. At -0.62 V all electrons reside in the lowest LL.

Once the charge density in the well has been deduced, the tunneling rate $(1/\tau_t)$ for electrons in the lowest subband can be calculated from the values of current density J and n_s^e at the peak of the resonance, since in equilibrium $J=n_s^e e/\tau_t$ as discussed first by Goldman *et al.* in Refs. 3 and 14, and subsequently employed in Refs. 7, 19, and 35.

Using $n_s=2.2\times10^{11}$ cm^{-2} deduced above, and $J=0.05$ A/cm^2 at the peak of the first resonance, a value for $\tau_t=0.7$ μsec is obtained, as deduced previously by Leadbeater *et al.*[18] for this structure from their magnetocapacitance results. At the first resonance, transport in this structure is believed to arise from tunneling between the two-dimensional electron gas in the emitter contact and the 2D states in the QW.[18,36]

Given the slow tunneling rate deduced above, slow compared to typical acoustic-phonon relaxation rates ($\sim10^8-10^9$ sec^{-1}) (Refs. 37 and 38) a thermalized electron distribution in the well, with temperature close to the lattice temperature, would be expected.

Evidence for the expected electron thermalization in the well at the first resonance is obtained from the present PL experiments. In magnetic field, tunneling occurs between the LL states in the emitter to those in the QW, with conservation of LL quantum number (n). At $B=4.3$ T, both $n=0$ and 1 LL's are populated in the emitter, where the sheet charge density is equal to 2.2×10^{11} cm^{-2} ($\nu=2.3$) throughout the resonance.[18] The fact that the $n=1$ LL in the QW is observed to depopulate at a bias of -0.62 V (Fig. 10) indicates clearly that electron thermalization in the well occurs before tunneling out, since tunneling into the $n=1$ LL must still arise from the populated $n=1$ LL in the emitter. Since electron scattering and hence thermalization occurs before tunneling out of the well, the tunneling process is sequential. The same conclusion was reached by Leadbeater *et al.* from their observations of magnetocapacitance oscillations from electrons in both the emitter and the QW.[19]

At the cutoff of the resonance at -0.68 V [Fig. 2(d)], the observation of a clear Fermi-energy feature indicates that the carrier temperature is $\lesssim 10$ K. However, at this bias the Fermi levels in the emitter and QW are equal, so a cold electron gas in the QW would be expected, as observed, irrespective of the importance of electron-energy relaxation process.

B. Second resonance

The splitting of the PL spectrum at -2.40 V into $n=0$ and 1 LL's is shown in Fig. 9. The intensity of the $n=1$ LL decreases strongly with increasing field up to ~7 T. However, in contrast to the first resonance, the $n=1$ LL is never observed to depopulate completely [Figs. 9(e) and 9(f)], even at 9.6 T. These results are presented in graphical form in Fig. 11, where the ratio of the $n=1$ to $n=0$ LL intensities (I_1/I_0) is plotted as a function of field (solid circles) together with similar results taken at -2.2 V (open circles). The long tail to high field of I_1/I_0 versus B is characteristic of an electron gas with elevated temperature of 25 to 40 K, as deduced earlier from the $B=0$ spectrum (Sec. III A). We obtain the best fit to the observed variation of I_1/I_0 against B at -2.4 V for $n_s^e=(3.2\pm0.3)\times10^{11}$ cm^{-2} ($E_F=11.1$ meV, $\nu=2$ at 6.7 T), $T=40$ K, and a rate of decrease of oscillator strength with energy a factor of 2 greater[39] than that employed to fit the zero-field spectrum of Fig. 2(g).[40] A similarly good fit for I_1/I_0 versus B at $V=-2.2$ V is obtained using other parameters the same as at -2.4 V, but for $n_s^e=1.9\times10^{11}$ cm^{-2} ($E_F=6.6$ meV, $\nu=2$ at 4.0 T). The increase of n_s^e of 1.3×10^{11} cm^{-2} between -2.2 and -2.4 V is close to that calculated for the change of n_s^e between -2.2 and -2.4 V of 1.2×10^{11} cm^{-2}, further supporting the reliability of the fitting procedure of Fig. 11. The increase in n_s^e is calculated from a parallel plate capacitor model on the reasonable assumption that all the additional charge associated with the increase in bias is located in the quantum well.

The constant ratio of I_1/I_0 between 8.3 and 9.6 T at -2.4 V is indicative of a higher electron temperature at 9.6 T than at 8.3 T.[37] This probably arises from the re-

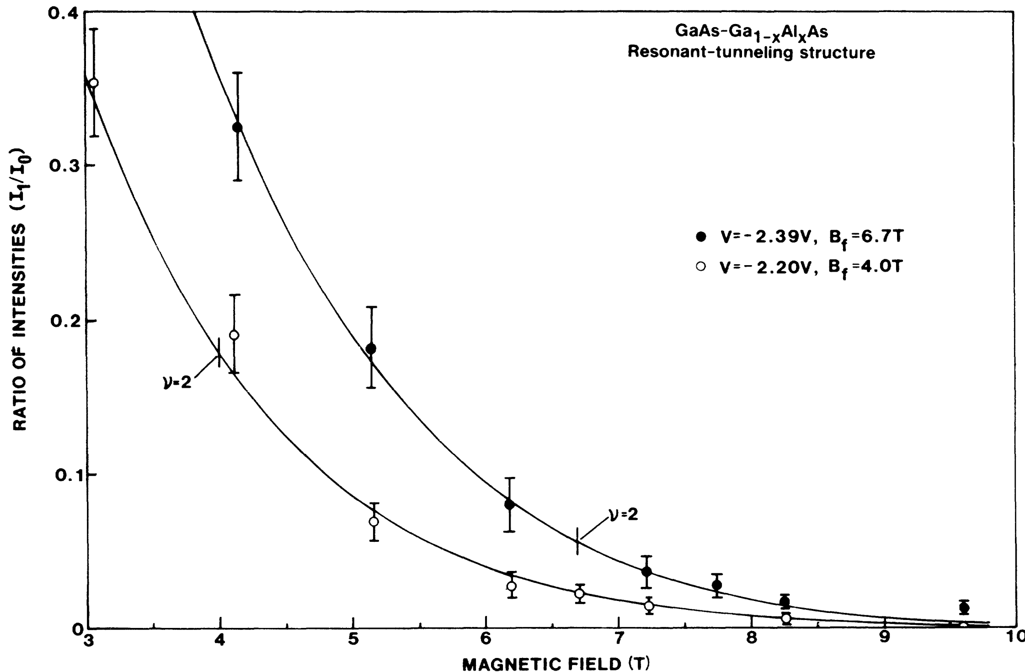

FIG. 11. Ratio of $n=1$ to $n=0$ Landau-level intensities as a function of magnetic field, at applied biases of -2.4 V (open circles) and -2.2 V (solid circles). The solid curves are fits ($T=40$ K) to the experimental points for fundamental fields B_f of 6.7 and 4.0 T, respectively. The fields at which $\nu=2$ at the two biases are indicated. The elevated electron temperature of 40 K is deduced from the long tails of the $n=1$ to $n=0$ LL intensities beyond $\nu=2$.

duced probability of the electron–acoustic-phonon energy relaxation mechanisms at high field. Qualitatively, this is expected since much larger phonon k vectors are needed to scatter between the quantized LL states at higher magnetic field values. An increasing electron temperature with magnetic field is probably the reason why the best fit to the $B=0$ spectrum in Fig. 2(g) is obtained for $T=25$ K, whereas the best fit to the I_1/I_0 ratio in Fig. 11 is found for $T=40$ K. However, it should be noted that in both cases reasonable fits to the spectra are still obtained for electron temperatures 5 K greater or lower than those quoted.

As discussed in Sec. IV, the electrons observed in PL at the second resonance tunnel into the upper subband and then scatter down to the lower subband by rapid LO-phonon emission (rate $\tau_i^{-1} \sim 10^{12}$ sec^{-1}), to an energy less than that of one LO phonon above the bottom of the band, before tunneling out of the well. The elevated electron temperature observed in the lower subband arises because the tunneling-out rate for electrons in the lower subband $(\tau^{-1})_1$ (calculated to be 10^9 sec^{-1} at -2.4 V) is of the same order or faster than the electron–acoustic-phonon relaxation rate τ_{ac}^{-1} of 10^8–10^9 sec^{-1}.[37,38] This situation contrasts with that found at the much lower applied bias of the first resonance where $(\tau^{-1})_1 \sim 1.4\times10^6$ sec^{-1}, and so the electrons cool to the lattice temperature before tunneling out of the well. It should also be noted that the electron temperature we observe of ~ 30 K at -2.40 V is in reasonable agreement with that found by Ryan *et al.*[37,38] and Polland *et al.*[41] for the temperature of a high-density photocreated electron gas in QW's, 200 to 400 psec after photoexcitation.

Clear LL features are not observed for structure 2, since the LL linewidth is of the order of the expected $n=0$ and 1 LL spacing where $\nu=2$ is reached. Nevertheless, the marked decrease of linewidth at -0.75 V between 0 and 5.4 T [Figs. 6(e) and 6(f)] is clear evidence of band filling for this structure at its second resonance. From the field at which a PL signal in the region of the $n=1$ LL is no longer discernible, we estimate a value for n_s^e of $(2.0\pm0.7)\times10^{11}$ cm^{-2} at -0.75 V.

C. PL linewidths in high magnetic field

As discussed earlier in this section, application of a quantizing magnetic field removes the free-carrier contribution to the PL linewidths. Under such conditions the residual PL linewidth is determined by inhomogeneous processes such as well width and alloy fluctuations. Lifetime broadening due to tunneling out of the well is negligible since tunneling rates $\sim 5\times10^{12}$ sec^{-1} would be required to explain the typical linewidths of ~ 3 meV, at least 3 orders of magnitude faster than tunneling rates for the lower subband in the present structures with relatively thick barriers.

The PL linewidths at a high magnetic field of 9.6 T, are plotted as a function of reverse bias in Figs. 1(c) and 5(c), for samples 1 and 2, respectively. The field is sufficiently high that the quantum limit is attained at all biases. The variations of PL linewidths with bias are much smaller

than at $B=0$, thus showing again that the principal contribution to the $B=0$ linewidths is that due to free carriers. Up to the onset of significant current flow on the second resonances at -2.0 V [Fig. 1(c)] and -0.5 V [Fig. 5(c)], there is very little change in the linewidths with bias.[42] However, within the second resonances, the PL linewidths are greater by up to ~ 1.5 meV than at lower biases, consistent with the poorer LL resolutions in Fig. 9 than in Fig. 8. The linewidths do not decrease when the structures switch down to the low-current states beyond the second resonances (when very similar linewidths are found at 0 and 9.6 T) nor are they bias dependent within the resonance, so it is very unlikely that the extra width is caused by electron or lattice-heating effects. Lattice-heating effects can be excluded additionally since we have found no change in linewidth for measurements made under pulsed bias conditions. For sample 2, at the onset of the sharp increase of linewidth at -0.5 V, observed at both 0 and 9.6 T, two poorly resolved PL peaks are visible, with the broader one, at ~ 2 meV to lower energy, taking over and becoming dominant beyond -0.55 eV. For sample 1, two peaks are not resolved, but the linewidths are clearly greater beyond -2.0 V. The reason for this behavior, possibly related to a change in carrier localization with n_s^e, is not clear at the present time. It is not a magnetic-field-dependent phenomenon, and is observed in apparently very similar forms for the two samples. The observations have some similarity to those found at the onset of current flow at the first resonances Sec. III A, but in those cases the relatively broad PL peaks were replaced by sharper peaks to lower energy [Figs. 2(a)–2(c), 6(a), and 6(b)].

These details of the PL process are certainly interesting, but are not relevant to the main point of the section, namely that the comparison of PL linewidths at $B=0$ and 9.6 T [Figs. 1(b), 1(c), 5(b), and 5(c)] allows a reliable identification of the effects of free-carrier broadening on the $B=0$ linewidths. It is also clear that a little caution must be exercised in interpreting an increase of linewidth at the onset of resonance purely in terms of charge buildup since other mechanisms can contribute to the broadening of the spectral lines. The most likely of these is broadening due to the presence of more than one emission line at resonance, such as we have observed in structures which show no detectable charge accumulation in magneto-PL experiments. In those instances we find an *abrupt* increase in linewidth at the onset of resonance, due to the presence of more than one poorly resolved emission line. The linewidth is then found to be almost independent of bias within the resonance. This is in marked contrast to the behavior when significant charge buildup does occur, for then the linewidth increases *continuously* throughout the resonance. The presence of more than one emission peak at resonance has been discussed above for structures 1 and 2, but in those cases additional large and strongly bias-dependent broadening due to free carriers was also demonstrated.

VI. CONCLUSIONS

A detailed photoluminescence study of charge-transport processes in GaAs-$Ga_{1-x}Al_xAs$ double-barrier resonant-tunneling structures has been reported. It has been shown that study of PL linewidths as a function of bias provides clear evidence for the occurrence of charge buildup in the structures on the tunneling resonances. This is confirmed by the observation of Landau-level structure in the PL spectra as a function of magnetic field. Line-shape fits to the PL spectra together with the study of the Landau-level populations with field provide reliable methods for the determination of the electron charge density in the wells. It has been demonstrated that study of the PL spectra in high magnetic field provides a direct method for the separation of free-carrier and inhomogeneous broadening contributions to the linewidths of the PL spectra.

In contrast to the conventionally employed transport measurements, photoluminescence investigations provide unambiguous information on the distribution of space charge, within and between subbands, which builds up in resonant-tunneling structures on resonance. As a result of these spectroscopic investigations, the tunneling has been shown to contain a major sequential component at both resonances for these structures with relatively thick barriers. The large density of electrons which builds up in the lower subband at the second resonances is found to have a temperature of 25 to 40 K, in contrast to the cold electron distribution found at the first resonances. This is consistent with the relatively fast ($\sim 5\times10^9$ sec^{-2}) tunneling rate in the lower subband at the bias of the second resonance, fast compared to typical acoustic-phonon relaxation rates.

ACKNOWLEDGMENTS

The work at Nottingham is supported by the United Kingdom Science and Engineering Research Council (SERC). One of us (P.E.S.) gratefully acknowledges financial support from SERC, the Australian Academy of Science and Technology, and the Royal Signals and Radar Establishment. We are very grateful to G. Hill and M. A. Pate for processing of one of the structures employed.

---

*Also at Department of Physics, University of Nottingham, Nottingham NG7 2RD, UK.

†Permanent address: Department of Physics, University of Wollongong, P.O. Box 1144, Wollongong, New South Wales 2500, Australia.

[1] R. Tsu and L. Esaki, Appl. Phys. Lett. **22**, 562 (1983); L. L. Chang, L. Esaki, and R. Tsu, Appl. Phys. Lett. **24**, 593 (1974).

[2] S. Luryi, Appl. Phys. Lett. **47**, 490 (1985).

[3] V. J. Goldman, D. C. Tsui, and J. E. Cunningham, Phys. Rev. B **35**, 9387 (1987).

[4] M. C. Payne, Semicond. Sci. Technol. **2**, 797 (1987).

[5]T. C. L. G. Sollner, W. D. Goodhue, P. E. Tannenwald, C. D. Parker, and D. D. Peck, Appl. Phys. Lett. **43**, 588 (1983).

[6]S. Sen, F. Capasso, A. Y. Cho, and D. Sivco, IEEE Trans. Electron Dev. **ED-34**, 2185 (1987).

[7]J. F. Young, B. M. Wood, G. C. Aers, R. L. S. Devine, H. C. Liu, D. Landheer, M. Buchanan, A. J. Springthorpe, and P. Mandeville, Phys. Rev. Lett. **60**, 2085 (1988).

[8]J. F. Young, B. M. Wood, G. C. Aers, R. L. S. Devine, H. C. Liu, D. Landheer, M. Buchanan, A. J. Springthorpe, and P. Mandeville, Superlatt. Microstruct. **5**, 441 (1989).

[9]W. R. Frensley, M. A. Reed, and J. H. Luscombe, Phys. Rev. Lett. **62**, 1207 (1989).

[10]J. F. Young, B. M. Wood, G. C. Aers, R. L. S. Devine, H. C. Liu, D. Landheer, M. Buchanan, A. J. Springthorpe, and P. Mandeville, Phys. Rev. Lett. **62**, 1208 (1989).

[11]D. G. Hayes, M. S. Skolnick, P. E. Simmonds, L. Eaves, D. P. Halliday, M. L. Leadbeater, M. Henini, and O. H. Hughes, Surf. Sci. (to be published).

[12]M. S. Skolnick, A. W. Higgs, P. E. Simmonds, D. G. Hayes, G. W. Smith, H. J. Hutchinson, A. D. Pitt, C. R. Whitehouse, L. Eaves, M. Henini, and O. H. Hughes, Surf. Sci. (to be published).

[13]An asymmetric DBRTS was first discussed by V. J. Goldman, D. C. Tsui, and J. E. Cunningham, Solid-State Electron. **31**, 731 (1988).

[14]The occurrence of intrinsic bistability in DBRTS due to charge buildup in the well on resonance and the resulting electrostatic feedback were first discussed by V. J. Goldman, D. C. Tsui, and J. E. Cunningham, Phys. Rev. Lett. **58**, 1256 (1987).

[15]For a discussion of the observations of Ref. 14 see comment by T. C. L. G. Sollner, Phys. Rev. Lett. **59**, 1622 (1987), reply by V. J. Goldman, D. C. Tsui, and J. E. Cunningham, *ibid.* **59**, 1623 (1987), and T. J. Foster, M. L. Leadbeater, L. Eaves, M. Henini, O. H. Hughes, C. A. Payling, F. W. Sheard, P. E. Simmonds, G. A. Toombs, G. Hill, and M. A. Pate, Phys. Rev. B **39**, 6205 (1989).

[16]A. Zaslavsky, V. J. Goldman, D. C. Tsui, and J. E. Cunningham, Appl. Phys. Lett. **53**, 1408 (1988); in *Proceedings of the 1st Conference on Electronic Materials, Tokyo, 1988* (Materials Research Society, Pittsburgh, 1989), p. 165.

[17]E. S. Alves, L. Eaves, M. Henini, O. H. Hughes, M. L. Leadbeater, F. W. Sheard, G. A. Toombs, G. Hill, and M. A. Pate, Electron. Lett. **24**, 1190 (1988).

[18]M. L. Leadbeater, E. S. Alves, L. Eaves, M. Henini, O. H. Hughes, F. W. Sheard, and G. A. Toombs, Semicond. Sci. Technol. **3**, 1060 (1988).

[19]M. L. Leadbeater, E. S. Alves, F. W. Sheard, L. Eaves, M. Henini, O. H. Hughes, and G. A. Toombs, J. Phys. Condens. Matter **1**, 10 605 (1989).

[20]F. W. Sheard and G. A. Toombs, Appl. Phys. Lett. **52**, 1228 (1988).

[21]D. A. B. Miller, D. S. Chemla, T. C. Damen, A. C. Gossard, W. Wiegmann, T. H. Wood, and C. A. Burrus, Phys. Rev. B **32**, 1043 (1985).

[22]An investigation of the PL excitation processes at $V=0$ and under reverse and forward biases will be reported separately, M. S. Skolnick and P. E. Simmonds (unpublished). A rate-equation analysis of the minority carrier recombination processes under a variety of biasing conditions will also be presented there.

[23]N. Vodjdani, F. Chevoir, D. Thomas, D. Cote, P. Bois, E. Costard, and S. Delaitre, Appl. Phys. Lett. **55**, 1528 (1989).

[24]M. S. Skolnick, J. M. Rorison, K. J. Nash, D. J. Mowbray, P. R. Tapster, S. J. Bass, and A. D. Pitt, Phys. Rev. Lett. **58**, 2130 (1987).

[25]C. Delalande, G. Bastard, J. Orgonasi, J. A. Brum, H. W. Liu, M. Voos, G. Weimann, and W. Schlapp, Phys. Rev. Lett. **59**, 2690 (1987).

[26]M. S. Skolnick, J. M. Rorison, K. J. Nash, and S. J. Bass, Surf. Sci. **196**, 507 (1988).

[27]M. K. Saker, M. S. Skolnick, P. A. Claxton, J. S. Roberts, and M. J. Kane, Semicond. Sci. Technol. **3**, 69 (1988).

[28]S.K. Lyo and E. D. Jones, Phys. Rev. B **38**, 4113 (1988).

[29]LO-phonon-assisted tunneling was first reported by V. J. Goldman, D. C. Tsui, and J. E. Cunningham, Phys. Rev. B **36**, 7635 (1987).

[30]M. L. Leadbeater, E. S. Alves, L. Eaves, M. Henini, O. H. Hughes, A. Celeste, J. C. Portal, G. Hill, and M. A. Pate, Phys. Rev. B **39**, 3438 (1989).

[31]R. Ferreira and G. Bastard, Phys. Rev. B **40**, 1074 (1989).

[32]A. Seilmeier, H. J. Hubner, G. Abstreiter, G. Weimann, and W. Schlapp, Phys. Rev. Lett. **59**, 1345 (1987).

[33]M. S. Skolnick, K. J. Nash, M. K. Saker, S. J. Bass, P. A. Claxton, and J. S. Roberts, Appl. Phys. Lett. **50**, 1885 (1987).

[34]C. Delalande, J. A. Brum, J. Orgonasi, M. H. Meynadier, G. Bastard, G. Weimann, and W. Schlapp, Superlatt. Microstruct. **3**, 29 (1987).

[35]L. Eaves, G. A. Toombs, F. W. Sheard, C. A. Payling, M. L. Leadbeater, E. S. Alves, T. J. Foster, P. E. Simmonds, M. Henini, O. H. Hughes, J. C. Portal, G. Hill, and M. A. Pate, Appl. Phys. Lett. **52**, 212 (1988).

[36]D. Thomas, F. Chevoir, P. Bois, E. Barbier, Y. Guldner, and J. P. Vieren, Superlatt. Microstruct. **5**, 219 (1989).

[37]J. F. Ryan, R. A. Taylor, A. J. Turberfield, and J. M. Worlock, Surf. Sci. **170**, 511 (1986).

[38]J. F. Ryan, R. A. Taylor, A. J. Turberfield, A. Maciel, J. M. Worlock, A. C. Gossard, and W. Weigmann, Phys. Rev. Lett. **53**, 1841 (1984).

[39]A similar study in a modulation-doped quantum well of 60-Å width and $n_s^e \sim 3\times10^{11}$ cm^{-2} also indicates that the rate of decrease of oscillator strength from $E=0$ to E_F is an increasing function of magnetic field [M. S. Skolnick (unpublished)]. In this case, of course, the electron temperature is equal to the lattice temperature of 2 K.

[40]It should be noted that the ratio I_1/I_0 plotted in Fig. 11 does not directly correspond to the ratio of the populations of the $n=1$ and 0 LL's. When account is taken of the decreasing oscillator strength with increasing energy employed in the fits of Fig. 11, a ratio of the $n=1$ to $n=0$ population of 0.09 is obtained at 8.25 T.

[41]H. J. Polland, W. W. Rühle, J. Kuhl, K. Ploog, K. Fujiwara, and T. Nakayama, Phys. Rev. B **35**, 8273 (1989).

[42]The relatively broad lines observed before the onset of the first resonances, probably arising from defect-related processes, are unaffected by magnetic field. Their widths are omitted from Figs. 1(c) and 4(c) for simplicity.